A molecular dynamics analysis of the mechanical effect of water on the deformation of silicon monocrystals subjected to nano-indentation

2005 Nanotechnology 16 15

(http://iopscience.iop.org/0957-4484/16/1/004)

INSTITUTE OF PHYSICS PUBLISHING NANOTECHNOLOGY
Nanotechnology **16** (2005) 15–20 doi:10.1088/0957-4484/16/1/004

A molecular dynamics analysis of the mechanical effect of water on the deformation of silicon monocrystals subjected to nano-indentation

C Y Tang and L C Zhang[1]

School of Aerospace, Mechanical and Mechatronic Engineering, The University of Sydney, NSW 2006, Australia

E-mail: zhang@aeromech.usyd.edu.au

Received 15 March 2004, in final form 2 September 2004
Published 30 November 2004
Online at stacks.iop.org/Nano/16/15

Abstract
This paper discusses the mechanical effect of water on the deformation of silicon monocrystals under nano-indentation with the aid of molecular dynamics analysis. The rigid TIP4P model was used to simulate the interactions between water molecules while the long-ranged non-bonded Lennard-Jones potential was applied for the pairs of unlike molecules. It was found that upon loading water molecules are lodged into the cavities of the silicon substrate, causing subsurface damage. The diamond cubic structure in the indentation zone transforms into an amorphous state with a body-centred tetragonal form (β-silicon) below the indentor. The presence of water significantly reduces the indentor–silicon adhesion that alters the structure of the residual deformation zone after complete unloading.

(Some figures in this article are in colour only in the electronic version)

1. Introduction

Nano-machining of silicon monocrystals plays an important role in the manufacture of microelectronic and semiconductor devices. In order to maintain a high surface integrity, water-based coolants are often used to ensure adequate heat dissipation in nano-machining processes such as nano-indentation, nano-scratching, nano-grinding and nano-polishing [1–3]. A study on the nano-wear of silicon [1] suggests that the nature of atomic bonding in the amorphous silicon layer depends on the extent of the effect of the normal sliding load. A later study on the comparison of various machining processes on silicon suggests that the damage and change of the subsurface structure of monocrystalline silicon is highly related to the effects of water in repeated nano-indentations [2]. It is shown that the retardation of property stabilization and the penetration of elements into the subsurface area might have taken place [2]. In this same study, the evidence of chemical reactions between the transformed silicon and the environment was not found.

Theoretical investigations on the nano-indentation of silicon showed phase transformations at the nanometre scale [4, 5]. A microstructural change from diamond cubic silicon to a crystalline tetragonal body-centred structure (β-silicon) occurs during loading of a diamond indentor. Upon unloading, the crystalline tetragonal form transforms into a disorderly amorphous silicon network. A subsequent study indicated that the presence of oxygen in the atmosphere would damage the subsurface structure of silicon [6].

On the other hand, nano-indentation on gallium arsenide (GaAs) under conditions of high atmospheric humidity showed that the area around the indentor exhibits substantial bulging similar to lateral cracking [7] and that by indenting tungsten in an HCl solution, the elastic behaviour of body-centred cubic metals is modified by a passivating layer. It was also demonstrated that the response of zirconia single crystals under micro-indentation is strongly related to the environmental conditions [8]. In a study of indentation-induced fracture of

[1] Author to whom any correspondence should be addressed.

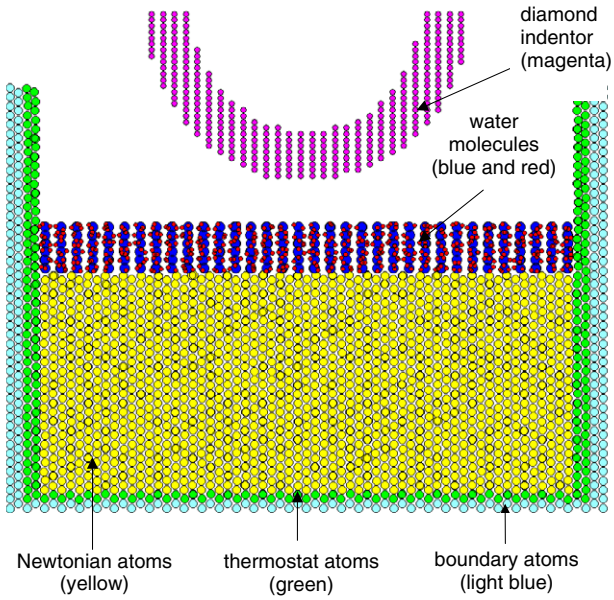

Figure 1. The initial molecular dynamics model for nano-indentation, showing silicon monocrystals, diamond indentor and water molecules. The water molecules consist of oxygen sites (bigger and darker dots) and hydrogen sites (smaller and lighter dots) based on the TIP4P model.

silicon, the standard deviation of crack lengths in toluene was found to be much smaller than those observed in air and water and this was attributed to enhanced plasticity [9].

The present study aims to investigate the mechanical effect of a water layer on silicon deformation under nano-indentation with the aid of molecular dynamics analysis.

2. Modelling and computational details

The diamond indentor, monocrystalline silicon (100) workpiece and water layer are shown in figure 1. The silicon substrate has the dimensions of 9.2 nm × 9.2 nm × 6.9 nm, located directly below the water layer. The silicon wall consists of boundary and thermostat atoms to prevent the overflow of water molecules and ensure adequate heat conduction in water. The entire model consists of 36 285 silicon atoms, 3906 carbon atoms of the diamond indentor and 3468 water molecules. The size of the model has been shown to be large enough so that boundary effects of the silicon walls can be ignored. The diamond indentor is initially positioned 13.2 Å above the silicon substrate and the initial configuration of water molecules has a depth of 12.3 Å.

A three-body Tersoff potential [10, 11], which has been extensively used in MD simulation studies of silicon [4], is used here to determine the interactions between the silicon atoms. The Morse potential [12] is applied to describe the interaction between the silicon and the inert diamond indentor. A rigid water model, TIP4P [13–15], is employed to describe the intra-molecular electrostatic and Lennard-Jones water interactions consisting of four interaction sites (two positively-charged hydrogen atoms, a non-charged oxygen atom and a negatively-charged site) located in a planar configuration. Molecular dynamics routines involving quartenions [14, 15] are used to determine the rotational motion of the rigid water molecules. Intra-molecular long-ranged electrostatics were not considered

Table 1. Parameters of the Lennard-Jones potential for unlike interatomic pairs.

Interatomic pair	ε (kJ mol^{-1})	δ (Å)
C–O	0.4785	3.275
Si (4-coordinated)–O	0.9286	3.388
Si (2-coordinated)–O	53.6616	1.3807

due to an insignificant role on the properties of silicon. The long-range Lennard-Jones potential, $\upsilon(r)$, is used to describe the non-bonded Si–H_2O and C–H_2O interactions as follows:

$$\upsilon(r) = 4\varepsilon[(\delta/r)^{12} - (\delta/r)^{6}] \tag{1}$$

where δ is a parameter determined by the equilibrium distance (distance of minimum energy) and ε is the potential depth determining the energy scale. These interactions are based on a C–O and Si–O inter-molecular potential without considering the hydrogen atom. The potential parameters used are given in table 1. The cutoff distance for these Lennard-Jones interactions are 8.1 and 6.0 Å respectively. This technique has been shown to be reliable in various molecular dynamics studies, such as those on water in carbon nanotubes [16–19], the nanoscale friction of alkyl monolayers [20] and on water confined in a cylindrical SiO_2 pore [21].

The Lorentz–Berthelot mixing rules [22] are used to approximate the Lennard-Jones parameters between pairs of unlike atoms in different molecules in equation (1), i.e.,

$$\delta_{xy} = \tfrac{1}{2} \times [\delta_x + \delta_y] \tag{2}$$

$$\varepsilon_{xy} = [\varepsilon_x \times \varepsilon_y]^{1/2} \tag{3}$$

where x and y represent silicon, carbon or oxygen atoms.

The oxidation of these water molecules is modelled via an orientation-independent Lennard-Jones potential between the silicon and oxygen atoms where the potential parameters are derived from a semi-empirical atom superposition and electron delocalization molecular orbital method [23]. In the present study, the coordination states of the top layer of silicon are assumed to be constant throughout the entire simulation.

The molecular simulations were run with multiple optimized time steps of 0.8 fs for water [14] and 2.5 fs for silicon [4] with an indentation speed of 40 m s^{-1}. Water was initially placed in a lattice configuration with a density of 0.997 g ml^{-1} and a temperature of 25 °C and the model was allowed to relax for 5000 time steps in order for the initial lattice structure to disintegrate. Experiments had shown that water typically displayed very limited adsorption on a silicon surface [24]. In the present study, nevertheless, a relatively thick water depth of 1.23 nm was chosen so that there was sufficient water–silicon contact in the interface throughout the nano-indentation. The diamond tool was initially positioned 5 Å above the top water layer and was indented downwards during the next 44 000 time steps. Unloading took place over the final 45 000 time steps. The method of carrying out the temperature–kinetic energy conversions was the same as that in [4], which had been shown to be reliable and accurate. No periodic boundary conditions were necessary. Two molecular dynamics simulations, one with and the other without a water layer, were conducted to understand the mechanical effect of water.

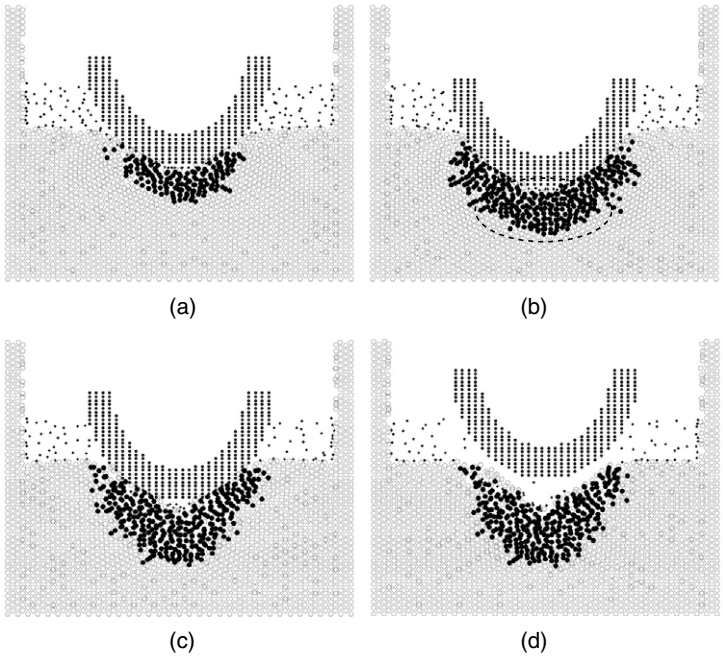

Figure 2. Cross-sectional views of deformation during nano-indentation with water where the small dots represent the oxygen sites in water molecules and solid circles represent six-coordinated amorphous silicon or higher. β-silicon is shown in the dashed circled region. The indentation depths are (a) $d = 1.58$ nm (loading), (b) $d = 2.58$ nm (loading), (c) $d = 1.58$ nm (unloading) and (d) $d = 0.58$ nm (unloading), respectively.

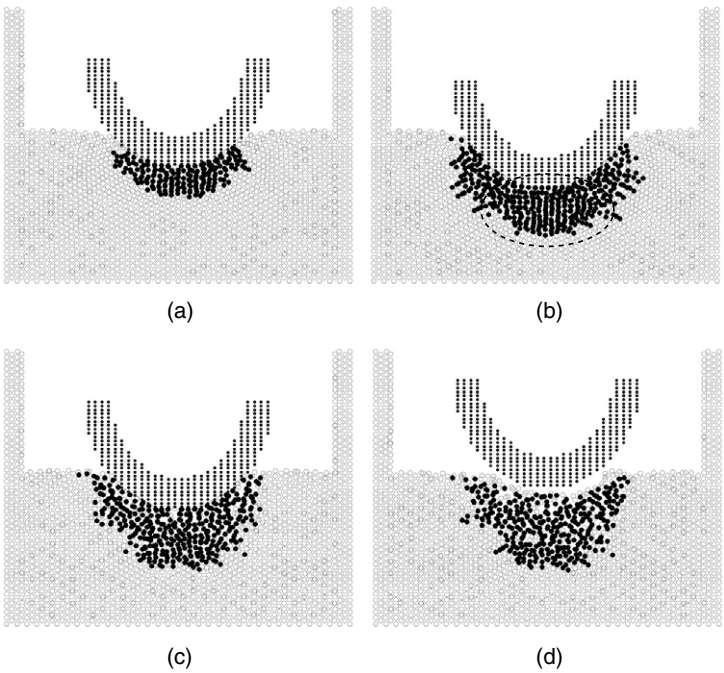

Figure 3. Cross-sectional views of deformation during nano-indentation without water. β-silicon is shown in the dashed circled area. The indentation depths are (a) $d = 1.58$ nm (loading), (b) $d = 2.58$ nm (loading), (c) $d = 1.58$ nm (unloading) and (d) $d = 0.58$ nm (unloading), respectively.

All simulations were run on a 127 node, 508 processor (1 GHz) Compaq Alphaserver SC [x1] and were performed with in-house developed classical molecular dynamic code written in Fortran 77. These simulations have been extensively tested for small perturbations in the initial conditions and thermodynamic parameters. The final simulation results are highly insensitive to these changes.

3. Results and discussion

3.1. Deformation characteristics

The indentation stages with and without water are shown in figures 2 and 3 respectively. For convenience of visualization, only the oxygen sites of water molecules are displayed. The inert diamond indentor and water molecules react repulsively

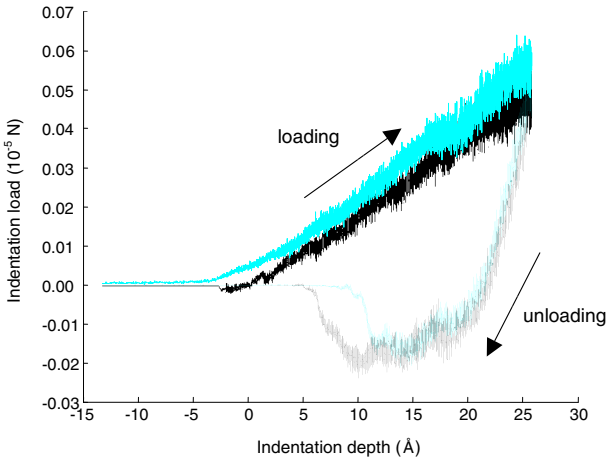

Figure 4. The load–displacement curves in a complete loading–unloading cycle ($d_{max} = 2.5786$ nm). The difference between the two curves at the end of unloading is due to the effect of water on the indentor–silicon adhesion.

via non-bonded van der Waals interactions so that water does not penetrate into the indentor. A small load is exerted onto the diamond indentor as the indentor starts to touch the water before contacting the silicon surface (figure 4). As the diamond indentor is pushed into the silicon, some water molecules are trapped at the indentation interface, thereby forming a cavity on the silicon surface (figure 2(a)). The damaged zone grows but the trapped water molecules do not penetrate further into the silicon subsurface (figure 2(b)). Upon unloading, the water molecules remain trapped and the cavity grows, hence forming a rough residual indentation mark (figures 2(c), (d)). On the other hand, when loading without water, the top layer of the silicon surface is always in contact with the indentor (figure 3(c)). Then after complete unloading, the surface of the residual indentation mark is much smoother. Recrystallization and elastic recovery occur due to the indentor–silicon adhesion. With water, the indentor–workpiece adhesion is considerably reduced. Thus upon unloading, less elastic recovery occurs within the indented zone and the shape of the indentation mark after complete unloading remains similar to that at the maximum indentation loading. The load–displacement curves (figure 4) show that the indentation load in water is higher throughout the indentation process. During unloading, the contact between the indentor and workpiece terminates earlier due to less adhesion. The two load–displacement curves show consistent variation relationships with the experimental findings at a larger scale [3]. The extent of the damage caused by water can be examined to a certain degree by considering the maximum depth of the residual mark. Upon unloading, the depth of this mark caused by the indentation with water (21.3 Å) is substantially higher than without water (11.8 Å). Clearly, water causes severer damage in the form of added indentation depth during loading while retarding elastic recovery during unloading.

3.2. Phase transformations

Transformation from diamond cubic silicon to β-silicon occurs during loading [4, 5]. This also occurs in both indentations, with and without water, as shown in figures 2(b)–(d), 3(b)–(d) and 5(b), which reveals that β-silicon grows during

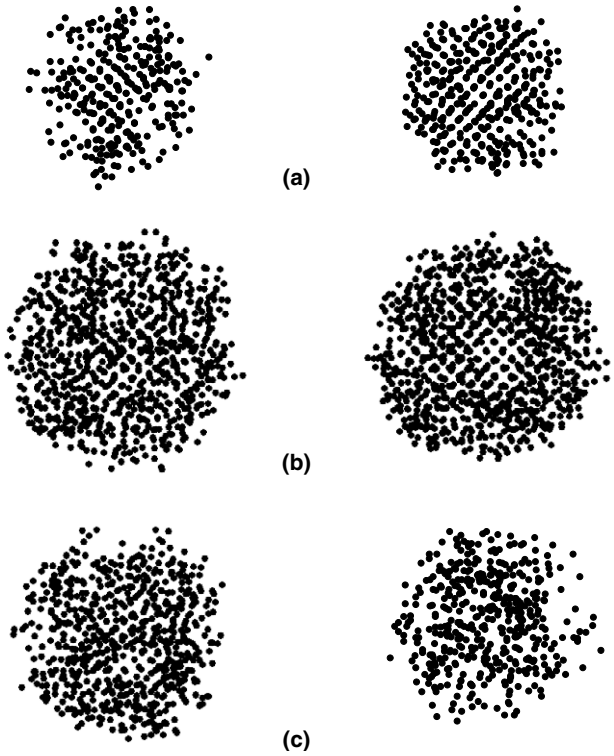

Figure 5. A bottom view of the growth of the amorphous region. The figures on the left and right represent the results with and without water, respectively. The growth and shrinkage of the β-silicon can be seen. The indentation depths are (a) $d = 1.58$ nm (loading), (b) $d = 2.58$ nm (loading) and (c) $d = 0.58$ nm (unloading), respectively.

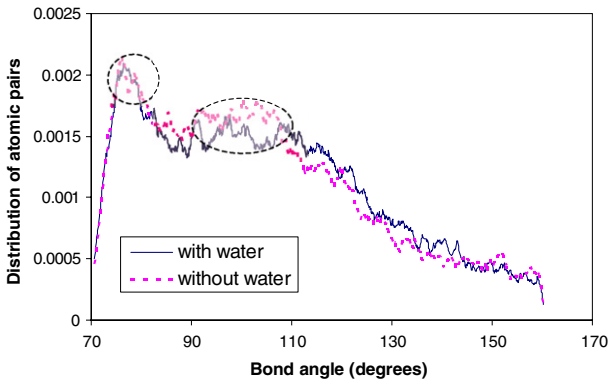

Figure 6. A comparison of the bond angles of amorphous silicon located in the indentation zone with and without water. The circled peaks are consistent with the theoretically expected values of β-silicon.

loading and disintegrates into an amorphous region upon unloading. With water, however, the development of the phase is limited to the zone just below the indentor tip (figure 2(b)). The amorphous volume shrinkage also becomes smaller (figure 5(c)). A comparison of the bond angles of closely packed six-coordinated atoms in the indentation zone (figure 6) reveals marked bond angle peaks that correspond to the theoretical values of crystalline β-silicon (76.9°, 93.9°, 105.2° and 149.5°) [25, 26]. The higher distribution of smaller bond angles in the simulation without water indicates a higher proportion of β-silicon in the transformed zone.

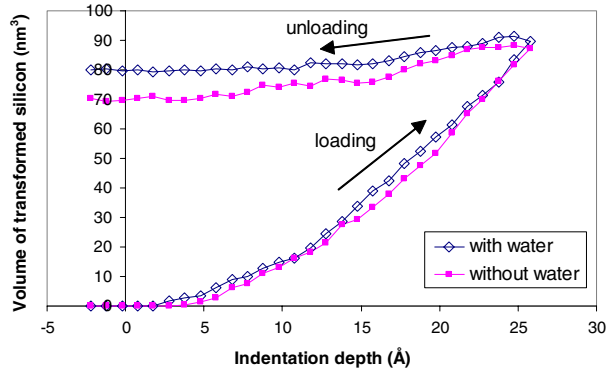

Figure 7. Number of transformed silicon atoms. The transformed zone is defined as the zone where the diamond cubic structure has transformed into other structures as well as atoms highly dislocated from their original positions.

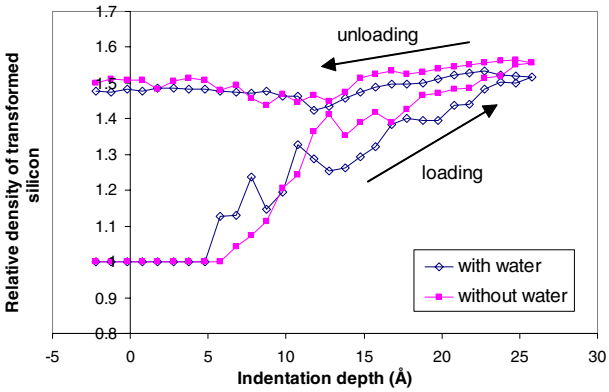

Figure 8. Relative density of transformed silicon versus indentation depth.

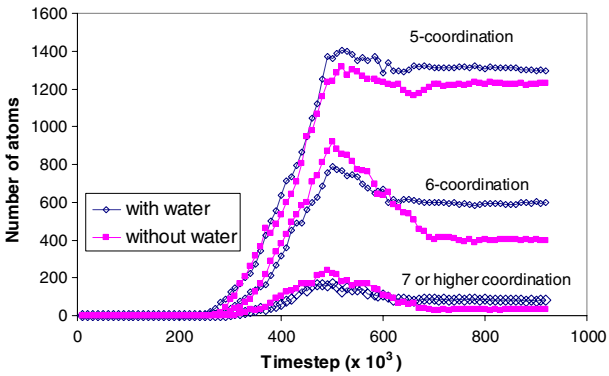

Figure 9. Structural changes of the substrate during nano-indentation with and without water.

Hence, because of the trapped water at the indentor–silicon interface, which alters the local stress distribution, the growth of β-silicon is retarded.

3.3. Microstructure and stress analyses

During nano-indentation with water, the volume of transformed silicon is found to be higher (figure 7). It seems that, during loading, water molecules behave as tiny moving surface indentors which penetrate into the silicon surface and modify the stress field in the neighbourhood, thereby

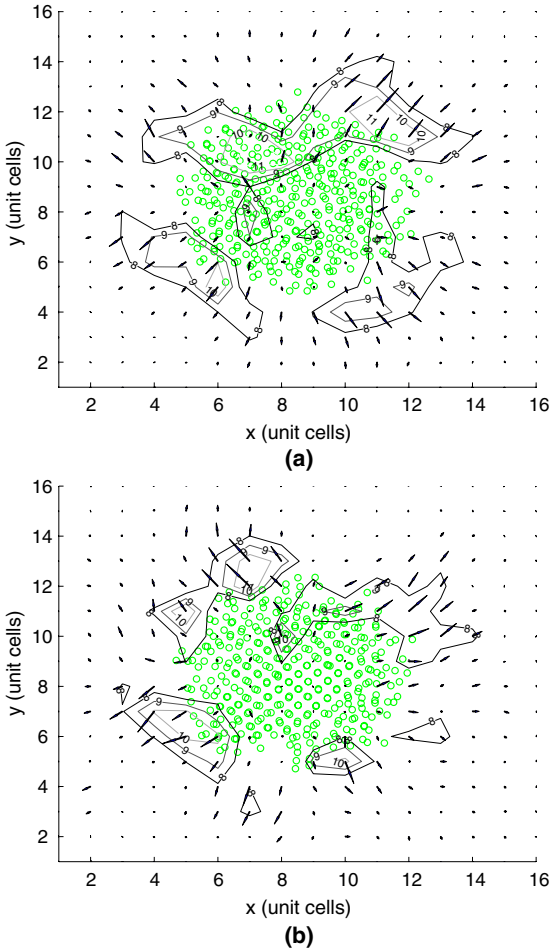

Figure 10. A comparison of stress fields at the maximum indentation load: (a) with water, and (b) without water. The contours (displaying stress levels over 8 GPa) represent maximum shearing stresses while the arrows indicate the direction and magnitude of the stresses. The light circles represent amorphous silicon with a coordination number equal to and higher than 6. The depth of the cross-section is $d = 2.85$ nm.

increasing the number and volume of the transformed silicon atoms. The recovery mismatch in the load–displacement curves (figure 4) indicates that the presence of a water layer reduces the indentor–silicon adhesive forces. This impedes the elastic recovery of the silicon, thereby resulting in a larger and deeper residual indent on the silicon sample. The phenomenon of moving surface asperities acting as abrasive grit was also noted in silicon nano-indentation with an oxygen molecule [6]. The density of the transformed silicon in the indentation without water is generally higher due to the higher formation of denser β-silicon (figure 8). The structural changes of the substrate summarized in figure 9 show that there is significant difference between the five- and six-coordinated silicon atoms in the cases with and without water. In the former, the number of six-coordinated atoms is higher at the maximum indentation, indicating a higher formation of β-silicon. The higher number of five-coordinated atoms represents a higher formation of non-crystalline amorphous silicon.

Figure 10 displays a comparison of the stress fields at the maximum indentation load with and without water at a cross-section at the depth of 2.58 nm in the subsurface. The trapped

water molecules at the indentation interface seem to have enlarged the zones of high shearing stresses. It is the change of these that altered the phase transformation details described above. It is clear that although the stress distributions in the two cases are similar, the magnitude and the sizes of the high stress zones are different.

4. Conclusions

This study has shown that the presence of a water layer in the nano-indentation of silicon has substantial mechanical effects in the form of different microstructural and deformation characteristics. In contrast to the situation of indentation without water, where β-silicon forms abundantly, the trapped water molecules at the indentation interface change the stress level in the subsurface and limit the transformation of β-silicon. The residual indentation marks become rougher. The mechanisms explored in this study explain some phenomena observed in relevant experiments [3].

Future work is needed to understand the chemical role of water molecules in the structural transformations.

Acknowledgments

The authors acknowledge the Australian Partnership for Advanced Computing National Facility (APAC) for support and provision of supercomputing facilities. The continuous financial support from the Australian Research Council (ARC) is very much appreciated.

References

[1] Zhang L C and Zarudi I 1999 *Wear* **225** 669–77
[2] Zarudi I, Zhang L C and Swain M V 2003 *Key Eng. Mater.* **233** 609–14
[3] Zhang L C and Zarudi I 2001 *Int. J. Mech. Sci.* **43** 1985–96
[4] Zhang L C and Tanaka H 1999 *JSME Int. J.* A **42** 546–58
[5] Cheong W C D and Zhang L C 2000 *Nanotechnology* **11** 173–80
[6] Mylvaganam K and Zhang L C 2002 *Nanotechnology* **13** 623–6
[7] Mann A B and Pethica J B 1996 *Langmuir* **12** 4583–6
[8] Pereira A S and Jornada J A 1994 *J. Mater. Res.* **9** 1059–62
[9] Masuda-Jindo K and Maeda K 1994 *Mater. Sci. Eng.* **176** 225–30
[10] Tersoff J 1986 *Phys. Rev. Lett.* **56** 632–5
[11] Tersoff J 1989 *Phys. Rev.* B **39** 5566–8
[12] Zhang L C and Tanaka H 1997 *Wear* **211** 44–53
[13] Jorgensen W L, Chandrasekhar J, Madura J D, Impey R W and Klein M L 1983 *J. Chem. Phys.* **79** 926–35
[14] Rapaport D C 1995 *The Art of Molecular Dynamics Simulation* (Cambridge: Cambridge University Press)
[15] Leach A R 2001 *Molecular Modelling* (Harlow: Prentice-Hall)
[16] Werder T, Walther J H, Jaffe R L, Halicioglu T and Koumoutsakos P 2003 *J. Phys. Chem.* B **107** 1345–52
[17] Koga K, Gao G T, Tanaka H and Zeng X C 2001 *Nature* **412** 802–5
[18] Koga K, Gao G T, Tanaka H and Zeng X C 2002 *Physica* A **314** 462–9
[19] van der Spoel D, van Maaren P J and Berendsen H J C 1998 *J. Chem. Phys.* **108** 10220–30
[20] Rovere M, Ricci M A, Vellati D and Bruni F 1998 *J. Chem. Phys.* **108** 9859–67
[21] Zhang L and Jiang S 2002 *J. Chem. Phys.* **117** 1804–11
[22] Allen M P and Tildesley D J 1987 *Computer Simulation of Liquids* (Oxford: Clarendon)
[23] Yang S and Kim H 1995 *Bull. Korean Chem. Soc.* **16** 1028–32
[24] Beaglehole D and Christenson H K 1992 *J. Phys. Chem.* **96** 3395–403
[25] Donohue J 1974 *The Structures of the Elements* (New York: Wiley) p 262
[26] Villars P and Calvert L D 1991 *Pearson's Handbook of Crystallographic Data for Intermetallic Phases* 2nd edn (Materials Park, OH: ASM International)